REVISTA MATÉRIA
V.24 N.03
ISSN 1517-7076 artículos e-12394, 2019

Estudio de las propiedades, estructurales, morfológicas y ópticas de nanopartículas de Cr_2O_3 sintetizadas por procesos de combustión de un solo paso y diferentes combustibles

Studies on structural, morphological, and optical properties of Cr_2O_3 nanoparticles: synthesized via one step combustion process by different fuels

Valeria Palermo [1], María Celeste Gardey Merino [2] ,
Patricia Vázquez [1], José Antonio Alonso [3],
Gustavo Romanelli [1], Mariana Rodriguez[2],
Silvina Lassa[4]

[1] CINDECA–CCT–CONICET - La Plata, Calle 47 N° 257, La Plata (B1900AJK), La Plata, Buenos Aires, Argentina.
[2] Grupo CLIOPE, Universidad Tecnológica Nacional - Facultad Regional Mendoza, Rodríguez 273, (5500), Mendoza, Mendoza, Argentina.
[3] Instituto de Ciencia de Materiales de Madrid (CSIC), Cantoblanco, 28049 Madrid, Madrid, Spain.
[4] MEByM - IANIGLA CONICET-Mendoza Av. Ruiz Leal s/n Parque Gral. San Martin, CC. 131, M5502IRA, Mendoza, Mendoza, Argentina.
e.mail: val_palermo@hotmail.com, mcgardey@frm.utn.edu.ar, ja.alonso@icmm.csic.es, silvina.lassa@gmail.com.

RESUMEN

Esta investigación presenta un nuevo método de síntesis de un solo paso para obtener Cr_2O_3 nanoestructurado a partir de una solución de nitrato de cromo y un combustible como ácido aspártico, o lisina, o trihidroximetilaminometano, o etilendiaminotetraacético. Una vez obtenido los polvos fueron calcinados a 500ºC. Luego se caracterizaron mediante difracción de rayos X (DRX), microscopía electrónica de barrido (MEB), microscopía electrónica de transmisión (TEM), espectroscopía infrarroja por transformada de Fourier (FTIR), espectroscopía por UV-Visible y técnicas de Brunauer–Emmett–Teller (BET). Estos polvos serán utilizados en superficies absorbedoras como cermts o pinturas selectivas solares. En las cenizas y los polvos calcinados obtenidos se identificó la estructura cristalina del Cr_2O_3, correspondiente al sistema romboédrico y al grupo espacial R-3c. El tamaño promedio de cristalita de los productos obtenidos estuvo entre 29 y 45 nm, donde para las cenizas el tamaño fue menor en comparación a los polvos obtenidos para todos los combustibles utilizados. Es probable que para un incremento de la temperatura el tamaño de cristalita crezca. Un área específica de 167 m^2/g fue determinada para las cenizas obtenidas con ácido aspártico. Este fue el mayor valor observado en la literatura específica y podría utilizarse para reacciones de catálisis, mientras que el resto de los valores obtenidos para las cenizas fue mayor en comparación a los polvos calcinados para todos los combustibles. El tamaño promedio de partícula observado a través de TEM resultó entre 50 y 100 nm aproximadamente. La energía de Band Gap determinada resultó entre 3.055 eV y 3.078 eV, esta variable aumenta suavemente con la temperatura de calcinación. Para confirmar esta tendencia se deberían realizar mayor cantidad de experimentos.

Palabras clave: Cr_2O_3, síntesis por combustión, energía de band gap.

ABSTRACT

This research presents a novel one–step solution combustion synthesis to obtain nano-structured Cr_2O_3 from chrome nitrate solution and one fuel such as aspartic acid (Asp) or Lysine (Lys), or trihydroxymethylamino-

Autor Responsável: María Celeste Gardey Merino Data de envio: 10/05/2018 Data de aceite: 31/08/2018

10.1590/S1517-707620190003.0707

methane (Tris) or ethylenediaminetetraacetic acid (Edta). Once obtained, the ashes were calcined at 500°C. The powders were characterized by x-ray diffraction (XRD), scanning electron microscopy (SEM), transmission electron microscopy (TEM), infrared spectroscopy with Fourier transform (FTIR), UV-Visible Spectroscopy (UV-VIS) spectroscopy and Brunauer–Emmett–Teller (BET) techniques. These powders will be used in solar absorbing surfaces: in composites (o cermets) and painted coatings. Within the obtained ashes and calcined powders, it was identified a Cr_2O_3 crystalline structure corresponding to the rhombohedral system and to the R-3c spatial group. The average crystallite size was determined for ashes and calcined powders, this value was in nanometric range between 29 and 45 nm, where for ashes were in general minor than calcined powders in all cases. It is probable that with an increment of the temperature, crystallite size would grow. A specific area of 167 m^2/g was determined for asp-ashes. This was a highest value observed in specific literature and it could be used in catalysis reactions, while the area values of ashes was higher than calcined powders value for each fuel. The average particle size observed through TEM resulted in 50 nm to 100 nm approximately. The determined Energy band gap resulted in 3.055eV to 3.078 eV approximately. The Energy band gap slightly increased with calcination temperature. Further trials and investigation will confirm the mentioned tendencies.

Keywords: Cr_2O_3, combustion synthesis, band edge energy

1. INTRODUCTION

Chromium Oxide (Cr_2O_3) is one of the most important wide band gap (Eg ≈ 3 eV) p-type semiconductor transition metal-oxide material. Cr_2O_3 is the most stable magnetic-dielectric oxide-material. It belongs to rhombohedral crystal system with lattice parameter a = b = 4.953 Å, c = 13.578 Å and space group R-3c (167). It expresses high electrical conductivity with partial or complete electron transfer. It is treated as an important refractory material because of its high melting temperature (≈2300 ◦C) and high temperature oxidation resistance [1].

Bulk Cr_2O_3 is an antiferromagnetic material with a Neel temperature of 307 K, whereas, nanostructured Cr_2O_3 shows magnetic properties that is due to the presence of uncompensated surface spins [2]. Magnetic nanoparticles have found numerous technological applications, one of the most important being data storage, as for example, hard disks in computers [3]. The titled compound Cr_2O_3 can also be used as an efficient gate-dielectric-material because it shows wide band gap, high melting temperature and high oxidation resistance, which is the essential requirement for a material to be used as gate-oxide materials [1]. Among various transition metal oxides that are prospective anodes for LIBs, Cr_2O_3 has been suggested as a promising candidate for anode electrode materials of the Li-ion battery due to its high theoretical specific lithium storage capacity (1058 mA h g^{-1}), relatively low lithium insertion potential among metal oxides (MOx) and low cost [4]. Additionally it is used as sensing electrodes [5] and catalysts for fluorination [6].

In principle there are several ways of achieving selective solar absorbing surfaces. The coatings are based on different optical absorption mechanisms including light trapping, particulate coatings, semiconductor-metallic layers, multilayer films, quantum size effects and intrinsic absorption. The most common absorber type is the absorber-reflector tandem. This absorber is obtained by combining two surfaces, one surface which is highly absorbing in the solar region and another highly reflecting in the infrared. They are two types of these absorbers where Cr_2O_3 could be stay as a component: composites (o cermets) and painted coatings. Composite coatings are surfaces consisting of small particles embedded in a dielectric matrix (also called cermet) deposited on a highly infrared reflecting metal substrate. The particles are usually transition metals embedded in an oxide matrix. The particles could either be uniformly distributed in the matrix or gradient index with decreasing content of the particles towards the front surface of the coating. These types of coatings have optical properties appropriate for selective solar absorbers [7]. Spectrally selective solar absorbers have also been extensively developed by sputtering. Cr–Cr_2O_3 cermets have been deposited by using Cr and Cr_2O_3 composite targets with radio frequency (RF) sputtering or using a single Cr target via reaction sputtering in an Ar + O_2 gas flow.[8]

Selective absorbing paints have the potential of being a less expensive alternative to the selectively solar-absorbing coatings. They can also be classified as the tandem type of absorbing particles uniformly distributed in a matrix deposited on a metal substrate. Their optical performance is governed by intrinsic optical constants as well as particle size-dependent scattering and absorption. As regards the absorption of the solar spectrum, the oxides of transition metals (Co, Mn, Fe and Cr) present a high absorbance owing to the existence of numerous, allowed, electronic transitions between their partially full “d” orbitals [9]. It has investigated paints having a variety of colours and spectral selectivity independent of the thickness of the deposited layer (TISS paint coatings). Such coatings would combine the advantages of paints (longevity, chem-

ical resistance achieved by a high thickness of the applied layer, variety of colors, simple application) with spectral selectivity. TISS paint coatings attained low emittance by the addition of metallic particles (aluminium or copper flakes), while other inorganic pigments impart them various colors [10]. The chromium (III) oxide (Cr_2O_3) material is being widely investigated nowadays due to its numerous application domains, including green pigments [11].

Various techniques have been developed for the synthesis of Cr_2O_3 nanoparticles, such as: thermal decomposition [11, 12], sol-gel [13-15], hydrothermal method [1, 5, 16-17], solvothermal method [3, 18], thermal process [19-21] microwave irradiation method [22], precipitation method [6, 23], magnetron-supttering [24], self-assembly-like method [8], precipitation–gelation method [25], and combustion solution method using glycine [4, 26-27] and ethylenediaminetetraacetic acid (Edta), as fuels [28]. The use of new fuels has not been found in specific literature.

Solution combustion synthesis is consistent with the following principles of Green Chemistry: N°3 design synthetic methods to use and generate substances that minimize toxicity to human health and the environment, N°5 minimized the use of auxiliary substances wherever possible and make them innocuous when used", N°6 minimize the energy requirements of chemical processes and conduct synthetic methods at ambient temperature and pressure if possible and N° 8 minimize or avoid unnecessary derivatization if possible, which requires additional reagents and generate waste [29]. By solution combustion syntheses, it is possible to obtain nanoparticles with homogenous crystalline structure by a one step, simple route. The parameters influencing combustion reactions include type of fuel, fuel to oxidizer ratio, use of an excess of oxidizer, ignition temperature and water content of the precursor mixture. The effect of fuel to oxidizer ratio in microstructure was studied in the synthesis of Co_3O_4 using urea as fuel; the influence of glycine and urea as fuels was studied to obtain Co_3O_4 through stoichiometric combustion syntheses and in studies for optimized combustion reaction to obtain Al_2O_3 with eight different fuels as lysine, glutamine and arginine etc [30].

This paper is aimed to present a novel one–step solution combustion synthesis to obtain nanostructured oxides from chrome nitrate solution and one fuel such as aspartic acid (Asp) or Lysine (Lys) or trihydroxymethylaminomethane (Tris) or ethylenediaminetetraacetic acid (Edta). Once obtained by combustion processes, the ashes were calcined at 500°C so as to get the powders containing the required crystalline structure. The powders were characterized by X-ray diffraction (XRD), scanning electron microscopy (SEM), transmission electron microscopy (TEM), infrared spectroscopy with Fourier transform (FTIR), UV-Visible Spectroscopy (UV-VIS) and Brunauer–Emmett–Teller (BET) techniques. This work is mainly focused on the comparison of the powders general properties before and after calcination as well as on the analysis of the relation between optical gap with the rest of the general properties like crystalline structure, average crystallite size, etc. Then these powders will be used as pigments for solar selective paints or in cermets in solar thermal collectors.

2. MATERIALS AND METHODS

2.1 Synthesis of powders

Cr_2O_3, powders have been obtained by combustion syntheses using $Cr(NO_3)_3.9H_2O$ and four different fuels; Asp, whose molecular formula is $C_4H_7NO_4$ Lys, $C_6H_{14}N_2O_2$, Edta, $C_{10}H_{16}N_2O_8$ and Tris, $C_4H_{11}NO_3$. All compounds are from Aldrich Company and pro-analysis (p.a).

In order to obtain a precursor the following components were dissolved in distilled water: 5g $Cr(NO_3)_3.9H_2O$ (Aldrich) and the quantity of fuels shown in Table 1.

PH-values of precursors corresponding to each fuel are indicated in Table 1**.** No precipitation was observed in any of the obtained precursors. The results were concentrated on a hot plate (HP) at 250 °C. When the remaining liquid was reduced enough, the combustion ignited with sparks and without flame in all cases. The resulting ashes were placed at 200 °C in a furnace for one hour to complete the reaction. Then, the ashes were exposed to a two-hour-calcination at 500 °C in air to remove organic compounds and obtain the rhombohedral crystalline structure. The samples were labeled as shown in Table1.

Table 1: Combustion synthesis parameters

NITRATES	FUELS	QUANTITY [G]	pH-SOLUTION PRECURSOR	ASHES SAMPLES	POWDERS SAMPLES
$Co(NO_3)_3.9H_2O$	Asp	1.66	3	Asp-ashes	Asp-powders
	Lys	1	4	Lys-ashes	Lys-powders
	Tris	1.83	5	Tris-ashes	Tris-powders
	Edta	1,37	3	Edta-ashes	Edta-powders

The selection of quantities for each fuel was carried out on the grounds of the following reactions for obtaining Cr_2O_3 as showed:

Asp: $2Cr(NO_3)_3 9H_2O + 2C_4H_7NO_7 \rightarrow Cr_2O_3 + 8CO_2 + 25H_2O + 4N_2$ (1)

Lys: $34Cr(NO_3)_3 9H_2O + 15C_6H_{14}N_2O_2 \rightarrow 17Cr_2O_3 + 90CO_2 + 411H_2O + 66N_2$ (2)

Tris: $14Cr(NO_3)_3 9H_2O + 10C_4H_{11}NO_3 \rightarrow 7Cr_2O_3 + 40CO_2 + 181H_2O + 26N_2$ (3)

Edta: $8Cr(NO_3)_3 9H_2O + 3C_{10}H_{11}N_2O_8 \rightarrow 4Cr_2O_3 + 30CO_2 + 96H_2O + 15N_2$ (4)

2.2 Characterization of powders

The phases contained in the resulting powders were identified by XRD using a Pan Analytical X'Pert PRO with a copper anode. Additionally, it was determined the average crystallite size from the width of Bragg peaks using Scherrer equation in the peak at $2\theta = 36°$. Diffraction data were analyzed by the Rietveld method [31], using the FULLPROF refinement program [32]. A pseudo-Voigt function was chosen to generate the line shape of the diffraction peaks. The following parameters were refined in the final runs: scale factor, background coefficients, zero-point error, pseudo-Voigt corrected for asymmetry parameters, isotropic thermal factors, and positional coordinates.

The powders morphology was observed through a JEOL, model 6610 LV microscope. The shape and size of the particles were observed by TEM with a JEOL 100 CX II (JAPAN, 1983) microscope using a voltage of 100 kV. FTIR plots were obtained by a Bruker IFS 66 and textural properties by BET technique with a Micromeritics Accusorb 2100. UV-visible spectra of aqueous solutions in quartz cuvettes were measured at room temperature with a Perkin Elmer Lambda 35 UV-vis double beam spectrophotometer, in the range 200-1100 nm at room temperature. This spectrometer uses tungsten and deuterium lamps to provide visible and UV wavelengths. Aqueous solutions were prepared using 50 mg of solid and 5 mL of distiller water. Although the samples were almost insoluble, the remaining solution, after the rest of solid material was removed, was used to measure the absorption spectra.

3. RESULTS AND DISCUSSION

By means of XRD, a Cr_2O_3 crystalline structure was identified in the obtained ashes (after combustion). Said structure is related to the rhombohedral system and R-3c spatial group. The X-ray diffraction diagrams are shown in Figure 1 and Figure 2 for ashes and powders respectively.

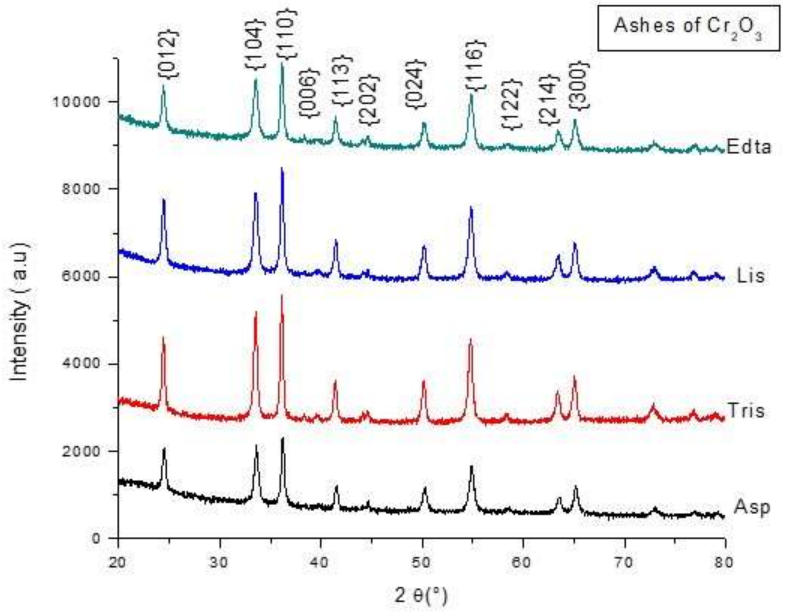

Figure 1: XRD of obtained ashes.

Crystalline structure consistent with the ICSD database [33] is shown in Figure 3. The presence of the required crystalline structure without calcination is an important contribution because the resulting process is simpler, economically convenient and of a lower environmental impact compared with the hydrothermal method [1], the sol-gel method [15] or the solution combustion method using Edta as fuel [28]. The presence of a phase in the ashes after combustion is due to the energy generated during combustion reactions of stoichiometric sufficient for the crystallization of Cr_2O_3, and Cr_2O_3 crystals can be easily obtained directly from the reaction of metal nitrates-Asp (Lys, Tris, or Edta) without further heating or calcined treatment [4]. Similar results were obtained using glycine as fuel [4]. As expected in all calcined powders after calcination at 500ºC, a Cr_2O_3 crystalline structure was observed, as seen in Figure 2. It is clear that the intensity of the diffraction peaks increased with temperature. This is due to that the higher temperatures could result in extensive crystallization. Furthermore, the nanopowder size was slightly increased with increasing temperature.

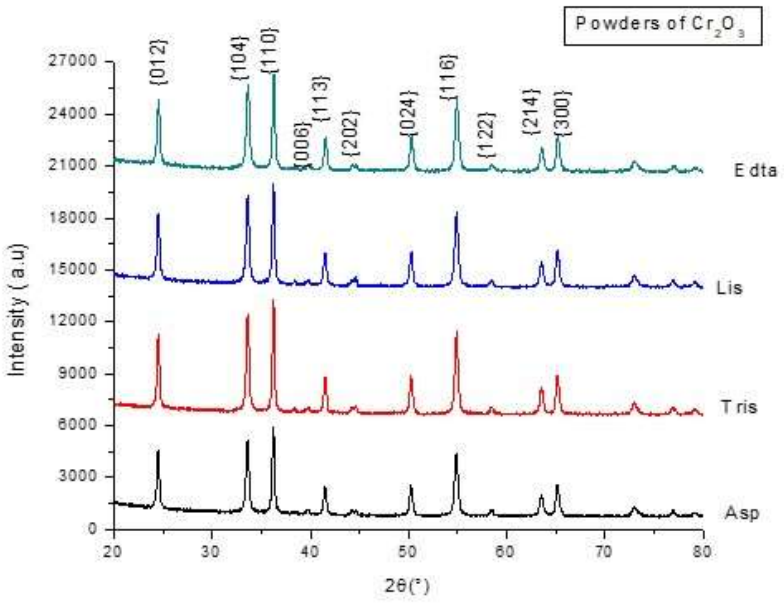

Figure 2: XRD of obtained powders.

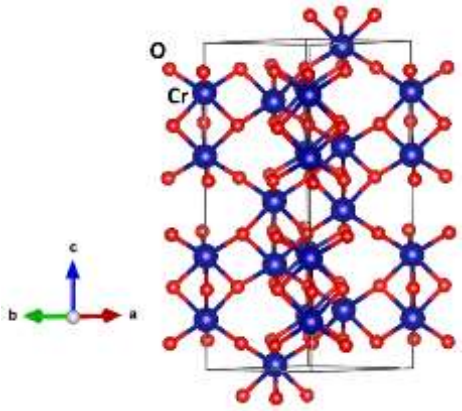

Figure 3: R -3c crystal structure observed in ashes and calcined powders in accord with Nº 75577 ICSD. Red spheres corresponding to oxygen atoms. Cr atoms are located in octahedral sites.

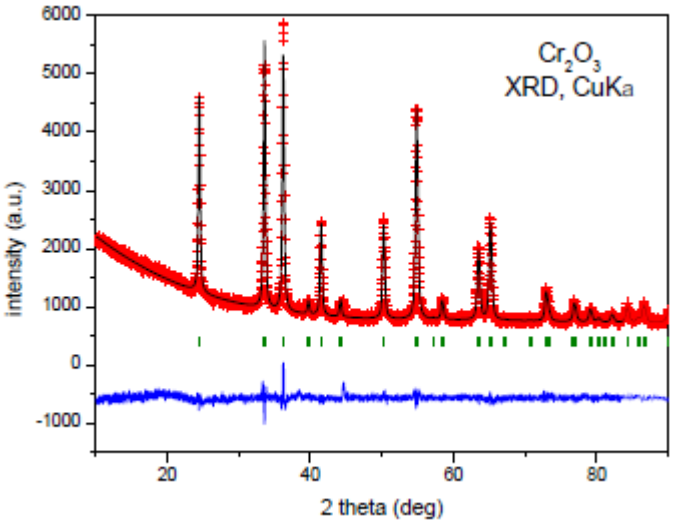

Figure 4: Observed (red crosses), calculated (black line) and difference (bottom line) XRD Rietveld profiles for Cr_2O_3 refined in R3-c space group. Corresponding to Asp-powders.

The Rietveld analysis allowed the refinement of the Cr_2O_3 crystal structure. It was defined a trigonal space group R-3c (Nº 161). We assumed that Cr atoms occupy the octahedral positions. A good agreement factors is obtained for this model with the, R_{Bragg}= 3.38%. An excellent fit was obtained between observed and calculated XRD profiles for this model (Figure 4). The most important structural parameters of Cr_2O_3, refined from XRD data at 25ªC are listed in Table 2 and Rietveld profile obtained is showed in Figure 4.

An average crystallite size determined for ashes and calcined powders resulting in nanometric range between 29 and 45 nm (Table 3). These results are coincident with those obtained through XRD diagrams (Figure 1 and Figure 2) where wide and low peaks, typical of nanostructured materials, are observed. In particular, crystallite size of ashes varies very little compared with calcined powders, resulting minor in all cases, except in Asp samples where both values were equal. Probably, with an increment of temperature, crystallite size would grow, as seen in Lys samples where crystallite grew from 24 to 40 nm. The range of values is similar compared with others in literature [3-4].

Table 2: Structural parameters of Cr_2O_3, refined from XRD data at 25ºC.

CRYSTAL DATA		
Trigonal, R-3c	X-ray CuKα radiation	
a = 4.9555 (2) Å	c = 13.5952 (7) Å	
V = 289.13 (2) Å^3	Z = 6	
REFINEMENT		
R_p = 3.14%	R_{wp} = 4.00%	
R_{exp} = 2.96%	R_{Bragg} = 3.38%	
χ^2 = 1.85		

FRACTIONAL ATOMIC COORDINATES AND ISOTROPIC DISPLACEMENT PARAMETERS (Å²)

	x	y	z	U_{iso}
Cr	0.00000	0.0000	0.34742(10)	0.3
O	0.3125(7)	0.0000	0.25000	0.3

As regards textural properties (see Table 3) like superficial specific area, the values of the ashes were higher than the value of the calcined powders for each fuel respectively. For instance, the area of Lys-ashes is 60 m^2/g. This value decreases to 5 m^2/g in Lys-powders. This fact could be related to an increase of particle and crystallite size. For Asp-ashes, a specific area of 167 m^2/g was determined. This value was the highest one observed in specific literature [3, 4, 6] and could be a very good candidate to be employed as catalyst in fluorination reactions [6].

Table 3: Textural properties obtained by BET Analysis and average crystallite size.

SAMPLE	SPECIFIC AREA [m²/g]	PORE VOLUME [cm³/g]	AVERAGE PORE DIAMETER [nm]	ISOTERMA TYPE	AVERAGE CRISTALLYTE SIZE [nm]
LIS-ASHES	60	0.147	9.81	IV H3	29
LIS-POWDERS	5	0.016	13.03		40
EDTA- ASHES	48	0.083	6.94		32
EDTA-POWDERS	32	0.113	14.25		45
TRIS- ASHES	17	0.045	10.65		40
TRIS-POWDERS	10	0.028	11.30		45
ASP- ASHES	167	0.433	10.4		45
ASP-POWDERS	27	0.136	20.9		45

In Figure 5, N_2 adsorption isotherms of Asp-ashes is shown, and is type IV [6] and H3 hysteresis loops according to the IUPAC classification corresponding to mesoporous materials (pore sizes between 2 to 50 nm) and coincident with the average pore width indicated in Table 1. Similar N_2 adsorption isotherms are observed in the rest of ashes and calcined powders. By solution combustion method using glycine as fuel were observed type IV isotherms and H2 hysteresis loops [3] and type III isotherms [25]. H3 hysteresis

loops is typical of porous materials composed of agglomerated particles in the form of sheets originating crack pores with a non-uniform size distribution. In fact, agglomerated particles in all calcined powders were observed in SEM micrographs (Figure 6). Particularly, Figure 6 a) presents a more compact morphology compared with the rest of the samples. In Figure 6 c) micrographs nano-metric particles and filaments (i.e minor at 1 μm), were identified, this is consistent with TEM micrographs of calcined powders presented in Figure 7 c). Similar superficial morphologies were observed in powders obtained by solution combustion synthesis [4].The morphologies of Cr_2O_3 catalysts prepared by solution combustion synthesis with glycine as fuel is formed in relatively uniform flakes or flat particles, while commercial Cr_2O_3 shows irregular particles with sizes ranging from 120 nm to 3 μm [26]. Chromium oxide nanoparticles have been synthesized using chromium nitrite and sodium oleate resulted in rice grain morphology an approximate length of 100 nm [2].

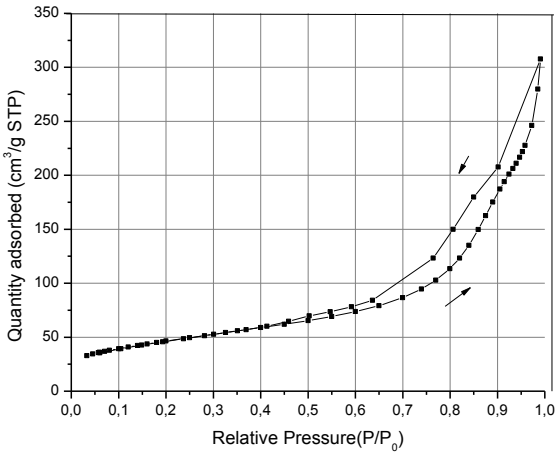

Figure 5:- N_2 adsorption isotherms Asp-ashes y Asp-powders

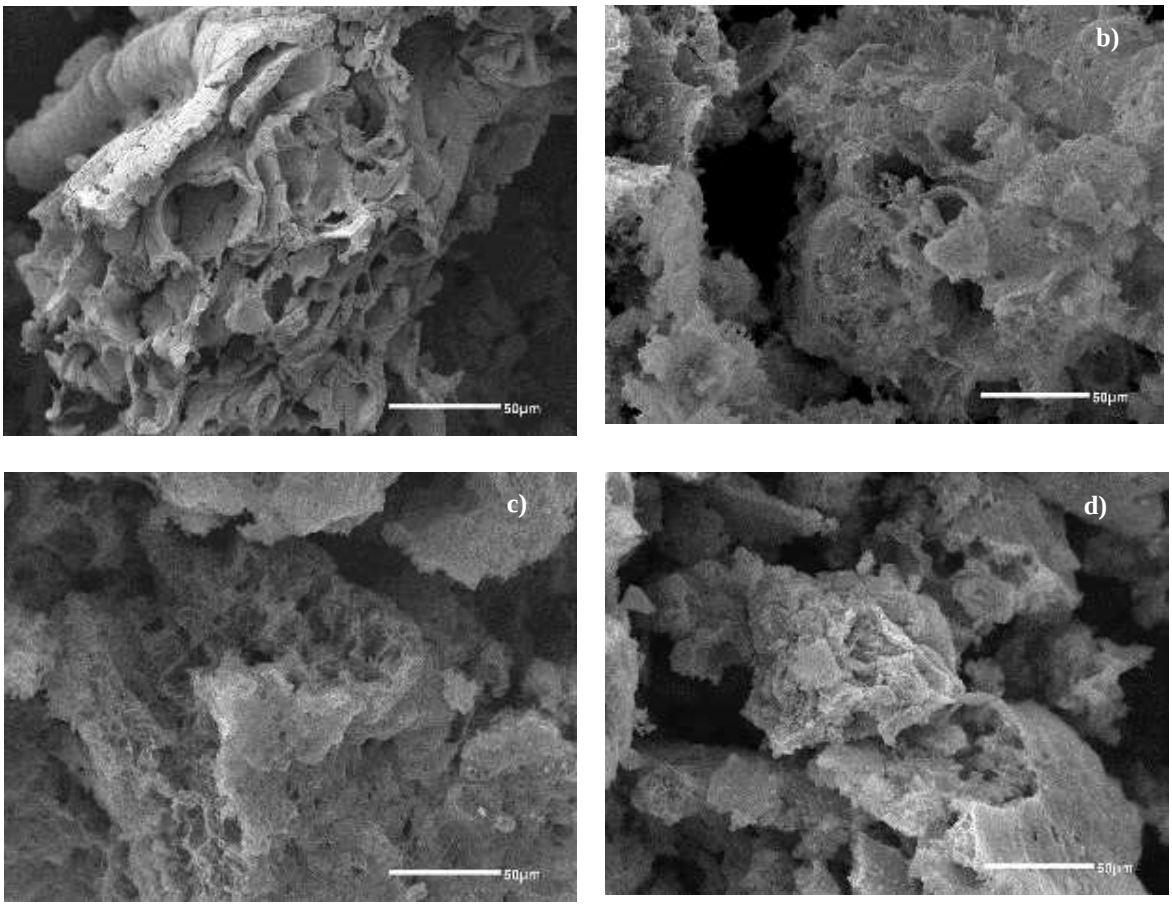

Figure 6: SEM Micrographs of calcined powders. a) Asp, b) Lis, c) Tris, d) Edta.

In Figure 7, TEM micrographs of calcined powders with a line scale of 20 nm are shown. Rounded edges, a circle form and large particles were observed in all samples with an average size of 50 to 100 nm approximately. Similar sizes were observed for particles obtained by thermal decomposition and subsequently used like pigments [11].

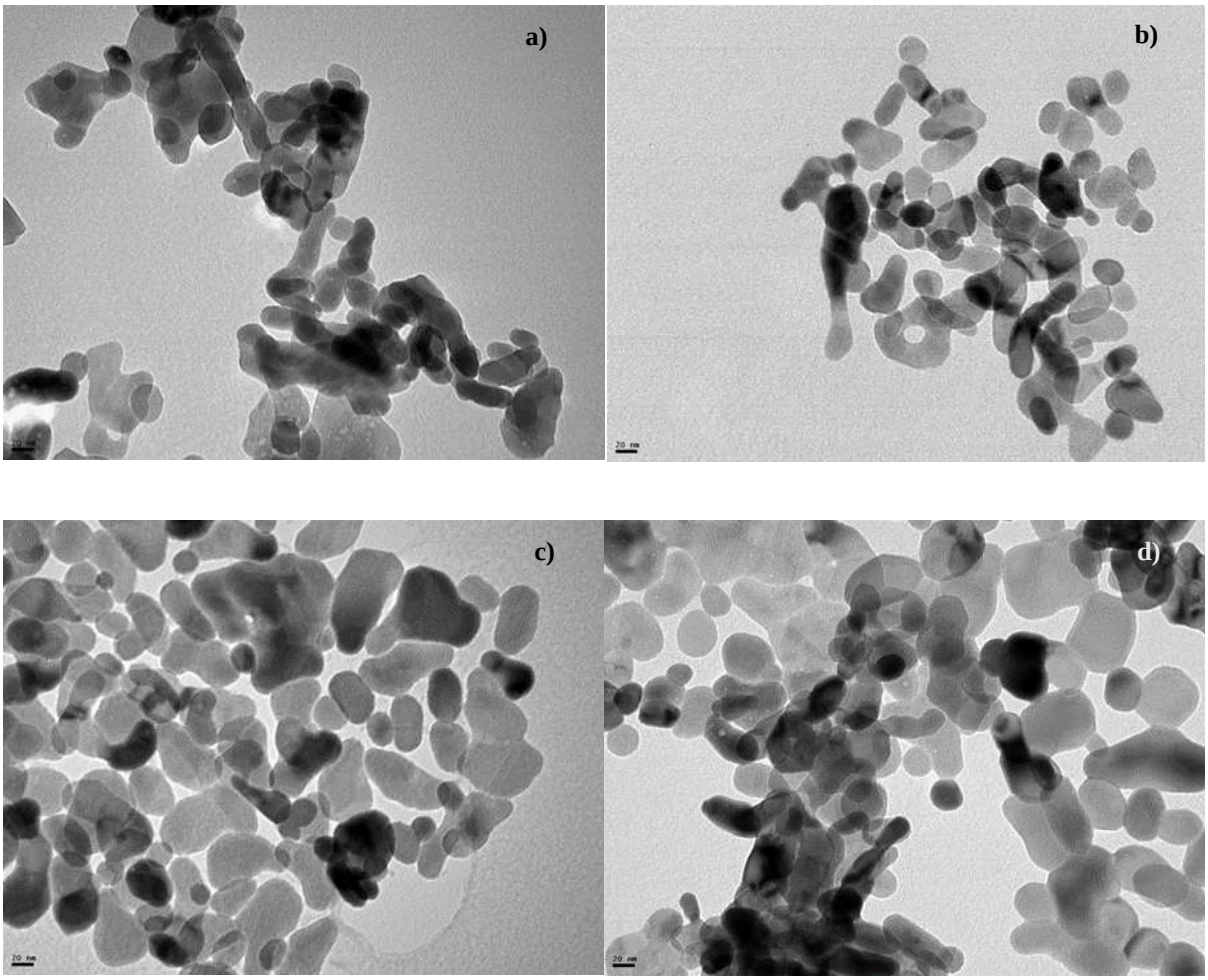

Figure 7: TEM Monographies of calcined powders - a) Asp, b) Lis, c) Tris, d) Edta.

FTIR spectroscopy is a useful tool to understand the functional group of ashes and obtained powders. In Figure 8, FTIR spectra of Lys-ashes (up) and Lys-powders (down) are presented. It was observed similar spectra in the rest of the powders. Metal oxides generally give absorption bands below 1000 cm^{-1} arising from inter-atomic vibrations. In the spectra, the bands that appeared at 713 y 547 cm^{-1} were attributed to the rhombohedral Cr_2O_3 structure [3]. The bands at 3430 cm^{-1} and 1647 cm^{-1} were assigned to adsorbed molecular water and hydroxyl groups, respectively. The absorption band at 2924 cm^{-1} was assigned to the intramolecular hydrogen bond derived from OH [28]. The 692 cm^{-1} peak is ascribed to the A_{2u} mode of α-Cr_2O_3. A_{2u} mode is a FTIR vibration mode which is a result of the structural symmetry in α- Cr_2O_3. The vibration band at 547 cm^{-1} characterizes the Cr–O distortion vibration and the band at 617 cm^{-1} identifies the chromium oxide as the Cr_2O_3 phase [28]. FTIR results show good coincidence with XRD analysis and indicate the successful production of pure Cr_2O_3 nanopowders. Similar FTIR spectra were observed in Cr_2O_3 powders obtained by solution combustion method using Edta as fuel [28].

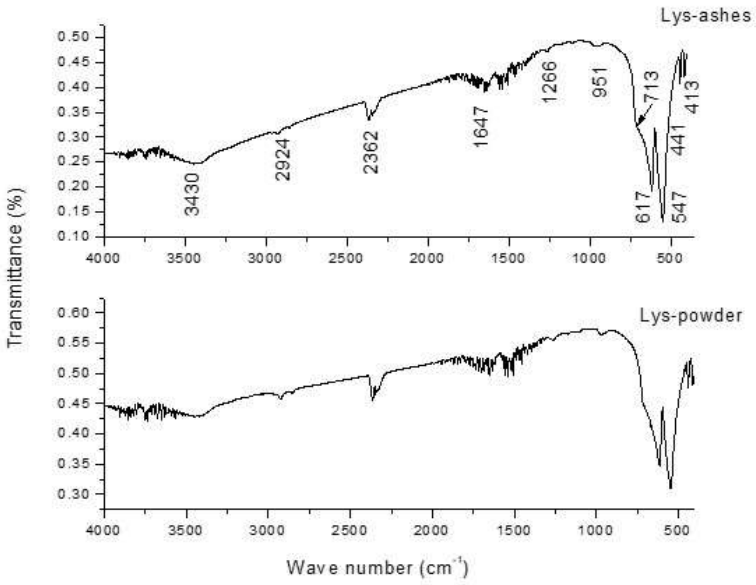

Figure 8: FTIR spectra of Lys-ashes and Lys-powders

The samples present absorption bands at 257 nm, 350 nm and a shoulder near 430 nm (Table 4). The band at 257 nm is attributed to oxygen-metal transfers [33, 34]. The absorption peak at 350 nm can be assigned to the band gap transition of the Cr^{+4} ions. The other peak centered at 450 nm correspond to the intrinsic $^4A_{2g}$-$^4T_{1g}$ d^3 electronic transitions of the Cr^{+3} ions situated in the six coordinate geometry and octahedral symmetry, based on the crystal field theory [35]. Table 4 shows Band Edge and Edge Energy of aqueous solution of Cr_2O_3.

The wavelength λ corresponding to Band Edge was calculated with the following equation:

$$\lambda = {}^{a}/_{-b} \qquad (5)$$

The absorption edge λ was defined by extrapolating the region of steep descent in the spectrum to zero, as shown in Figure 10. Romanelli et al. successfully employed this methodology to determine the optical band gap in heteropolyacid solutions [37]. The Energy edge represents the transfer of an electron from the Highest Occupied Molecular Orbital (HOMO) to the lowest unoccupied molecular orbital (LUMO). This energy gap was consistent with the reduction potential: the most reducible sample showed the smallest energy gap between the HOMO and the LUMO [38].

Edge energy (***E***) was calculated from the absorption edge wavelength by $\boldsymbol{E = hc/\lambda}$, where ***h*** is Planck's constant and *c* is the speed of light. The determined Energy band gap (*see* Table 4) resulted between 3.055 and 3.078 eV approximately and these values are in concordance with the reported ones, measured with a NIR spectrophotometer (≈ 3.2 eV) [1]. The use of UV–visible spectroscopy of aqueous solution in contact with Cr_2O_3 could be a simple diagnostic of the redox properties. As regards fuel influence and calcination temperature, some differences were observed in the second decimal place. With respect to temperature influence, the calcined powders have an energy Edge slightly higher compared to the ashes for the same fuel, except for powders obtained with Asp. This is a general indicator that the energy band gap increases with temperature. The highest band gap could be also because of cristallinity structure change. A high band gap is the essential requirement for a material to be used as gate-oxide materials [1]. Oxides obtained by a technique assisted with surfactants achieve band gap energy of 3.78; 3.72 and 3.68 eV [36].

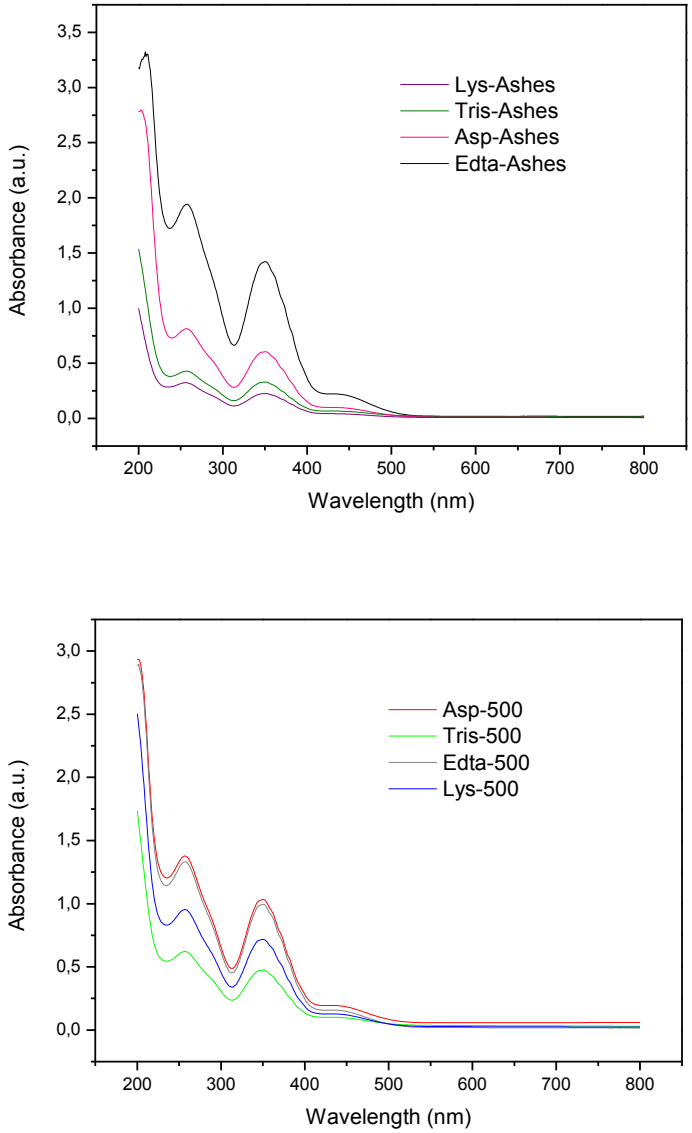

Figure 9: Absorption spectra of aqueous solutions: (up) powders, (down) ashes.

Table 4: Band Edge and Edge Energy of aqueous solution of Cr_2O_3.

SAMPLE	A	B	BAND EDGE (λ) (nm)	EDGE ENERGY (E) (eV)
LIS-POWDER	4.97	-0.012	414.02	3.076
LIS-ASHES	1.55	-0.003	416.90	3.055
EDTA-POWDER	6.80	-0.016	414.47	3.073
EDTA ASHES	9.70	-0.023	415.15	3.068
TRIS-POWDER	3.26	-0.008	415.22	3.067
TRIS-ASHES	2.26	-0.005	415.66	3.064
ASP-POWDER	7.14	-0.017	414.87	3.070
ASP-ASHES	4.20	-0.010	413.75	3.078

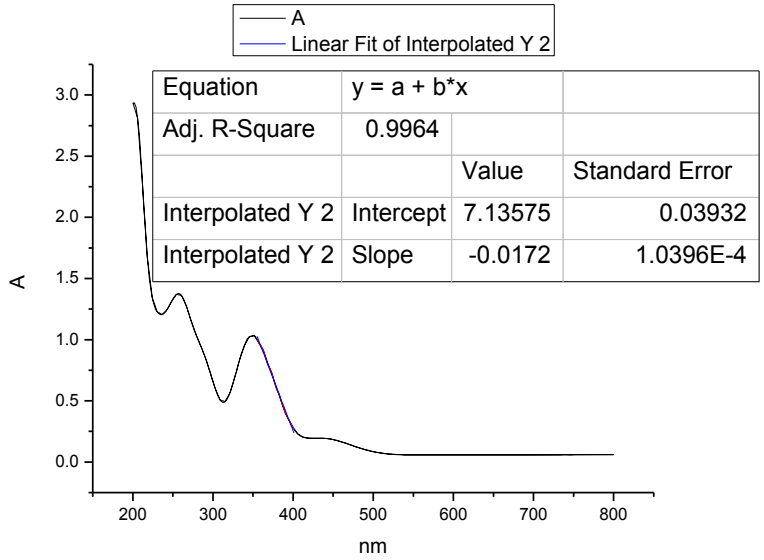

Figure 10: UV-visible spectrum of aqueous Asp-powder solution.

4. CONCLUSIONS

Cr_2O_3 nano-structured powders have been obtained by a novel one–step solution combustion synthesis combining chrome nitrate solution and different fuels. One of the original aspects about this investigation is the formation of Cr_2O_3 crystalline structure in the obtained ashes from combustion with and without calcination at high temperatures. The resulting crystallite average size was of a nano-metric range, between 29 and 45 nm. With respect to textural properties, superficial specific area, for ashes obtained with Asp resulted in 167 m^2/g, the highest value found in specific literature that could be used in catalysis reactions. Energy band gap values ranged between 3.055 and 3.078 eV. Energy band gap slightly increased with the calcination temperature. Further trials would be necessary to confirm these tendencies. A high band gap is the essential requirement for a material to be used as gate-oxide materials.

5. ACKNOWLEDGEMENTS

We want to acknowledge granting number UTN 2318 from National Technological University for their support and PICT 2014-3175 from FONCYT Argentina.

6. BIBLIOGRAPHY

[1] ABDULLAH M. M., RAJAB F. M, AL-ABBAS S. M., "Structural and optical characterization of Cr_2O_3 nanostructures: Evaluation of its dielectric properties", *AIP Advances* v. 4, pp. 027121 1- 027121, 2014.

[2] GUPTA, R.K., MITCHELL, E., CANDLER, J., *et al*., "Facile synthesis and characterization of nanostructured chromium oxide", *Powder Technology* v. 254, pp. 78–81, 2014.

[3] ANANDAN, K., RAJENDRAN, V., "Studies on structural, morphological, magnetic and optical properties of chromiums esquioxide (Cr_2O_3) nanoparticles: Synthesized via facile solvothermal process by different solvents", *Materials Science in Semiconductor Processing*, v. 19, 136–144, 2014.

[4] CAO, Z., QIN, M., JIA, B., *et al*., "Facile route for synthesis of mesoporous Cr_2O_3 sheet as anode materials for Li-ion batteries", *Electrochimica Acta* v.139, pp. 76–81, 2014.

[5] PEI Z., PEI, J., CHEN, H., GAO, L., *et al*., "Hydrothermal synthesis of large sized Cr_2O_3 polyhedrons under free surfactant", *Materials Letters*, v. 159, pp. 357–361, 2015.

[6] XIE, Z., FAN, J., CHENG, Y., *et al*., "Cr_2O_3 Catalysts for Fluorination of 2‑Chloro-3,3,3-trifluoropropene to 2,3,3,3-Tetrafluoropropene", *Industrial and Engineering Chemical Research*, v. 52, pp. 3295−3299, 2013.

[7] TESFAMICHAEL, T., "Characterization of selective solar absorbers experimental and theoretical modeling". ISSN 1104-232X, ISBN 91-554-4772-4. *Sweden by University Printers, Uppsala (2000). http://uu.diva-portal.org/smash/get/diva2:160605/FULLTEXT01*.

[8] CAO, F., MCENANEY, K., CHEN, G., *et al*., "A review of cermet-based spectrally selective solar absorbers", *Energy Environment Science*, v. 7, pp. 1615–1627, 2014.

[9] VINCE, J., ŠURCAVUK, A., OPARA KRAŠOVEC, U., *et al*., "Absorber coatings based on CoCuMnOx spinels prepared via the sol-gel process: structural and optical properties", *Solar Energy Materials and Solar Cell*, v. 79, pp. 313-330, 2003.

[10] OREL, B., SPREIZER, H., SLEMENIK PERŠE, L., *et al*., "Silicone-based thickness insensitive spectrally selective (TISS) paints as selective paint coatings for coloured solar absorbers (Part I)", *Solar Energy Materials & Solar Cells*, pp. 93–107, 2007

[11] GIBOT P., VIDAL L., "Original synthesis of chromium (III) oxide nanoparticles", *Journal of the European Ceramic Society*, v. 30, pp. 911–915, 2010.

[12] JANKOVSKÝ, O., SEDMIDUBSKÝ, D., SOFER, Z., *et al*., "Simple synthesis of Cr_2O_3 nanoparticles with a tunable particle size", *Ceramics International*, v. 41,n. 3, B, pp. 4644-4650, 2015 .

[13] CAO, H., QIU, X., LIANG, Y., *et al*., "Sol-gel synthesis and photoluminescence of *p*-type semiconductor Cr_2O_3 nanowires", *Applied Physics Letters*, v. 88, pp. 241112,1- 241112,3, 2006.

[14] BALOURIA, V., SINGH, A., DEBNATH, A., *et al*., "Synthesis and Characterization of Sol-Gel Derived Cr_2O_3 Nanoparticles", *Solid States Physics, AIP Conference Procedia*, v. 1447, pp. 341-342, 2012.

[15] AFZAL, A., ATIQ, S., SALEEM, M., *et al*., "Structural and magnetic phase transition of sol–gel-synthesized Cr_2O_3 and $MnCr_2O_4$ nanoparticles", *Journal of Sol-Gel Science and Technology*, DOI 10.1007/s10971-016-4066-4.

[16] RAJAGOPAL, S., BHARANESWARI, M., NATARAJ, D., *et al*., "Crystal structure and electronic properties of facile synthesized Cr_2O_3 nanoparticles", *Materials Research Express*, v. 3, pp. 095019,1-095019,10, 2016.

[17] PARDO, P., CALATAYUD, J. M., ALARCÓN, J., "Chromium oxide nanoparticles with controlled size prepared from hydrothermal chromium oxyhydroxide precursors", *Ceramics International*, v. 43, n. 2, pp. 2756-2764, 2017.

[18] ROY, M., GHOSH, S., KANTI NASKAR, M., "Solvothermal synthesis of Cr_2O_3 nanocubes via template-free route, *Materials Chemistry and Physics*, v.159, pp. 101-106, 2015.

[19] CHEN, Z., DUN, Y., LI, Z., *et al*., "Synthesis of black pigments containing chromium from leather sludge", *Ceramics International*, v. 41, n. 8, pp. 9455-9460, 2015.

[20] IBARRA-GALVÁN, V., LÓPEZ-VALDIVIESO, A., VILLAVELAZQUEZ-MENDOZA, C. I., *et al*., "Synthesis of Eskolaite (α-Cr_2O_3) Nanostructures by Thermal Processing of Cr_2O_3-Loaded Activated Carbon", *Particulate Science and Technology: An International Journal*, v. 32, n. 5, pp. 451-455, 2014.

[21] HAN LI, B., HAN YU, T., YU WENG, C., *et al*., "Thermal and plasma synthesis of metal oxide nanoparticles from MOFs with SERS characterization", *Vibrational Spectroscopy*, v. 84, pp. 146–152, 2016.

[22] BABU, I. M., WILLIAM, J. J., MURALIDHARAN, G., "Cr_2O_3 Nanoparticles: Advanced Electrode Materials for High Permormance Pseudocapacitors", *DAE Solid State Physics Symposium AIP Conference Procedia*, v. 1832, pp. 050017-1 to 050017-3, 2016.

[23] ZHAO, W., ZHANG, H., LIU, J., *et al*., "Preparation of Cr_2O_3 nanoparticles via surfactants-modified precipitation method and their catalytic effect on nitridation of silicon powders", *Journal of the Ceramic Society of Japan*, v. 20177, pp. 2623-2627, 2017.

[24] TEIXEIRA, V., SOUSA, E., COSTA, M.F., *et al.*, "Spectrally selective composite coatings of Cr-Cr_2O_3 and Mo-Al_2O_3 for solar energy applications", *Thin Solid Films*, v. 392, pp. 320-326, 2001.

[25] WOOK KIM, D., SHIN, S-IL., LEE, J-DAE, *et al*., "Preparation of chromia nanoparticles by precipitation–gelation reaction", *Materials Letters*, v. 58, pp. 1894-1898, 2004.

[26] HAN, W., WANG, Z., LI, X., *et al*., "Solution combustion synthesis of nano-chromia as catalyst for the dehydrofluorination of 1,1-difluoroethane", *Journal Material Science*, v. 51, n. 24, pp. 11002–11013, 2016.

[27] LIMA, M.D., BONADIMANN, R., ANDRADE, M.J., *et al*., *Journal of the European Ceramic Society*, v.26, pp. 1213–1220, 2006.

[28] AGHAIE-KHAFRI, M., LAFDANI, M.H.K., "A novel method to synthesize Cr_2O_3 nanopowders using EDTA as a chelating agent", *Powder Technology*, v. 222, pp. 152–159, 2012.

[29] ANASTAS, P.T., WARNER, J.C., *Green Chemistry: theory and practice, Ed. S. Publications, Oxford University Press, N. York, U.S.A.*, 1988.

[30] https://www.academiapublishing.org/journals/ajsr/pdf/2016/Oct/Merino.pdf, 08/ 03/ 2017.

[31] RIETVELD, H. M., "A profile refinement method for nuclear and magnetic structures, Journal of Applied Crystallography", v. 2, pp. 65-71, 1969.

[32] RODRIGUEZ-CARVAJAL, "Recent advances in magnetic structure determination by neutron powder diffraction", *Journal Physica B*, v. 192, pp. 55-69, 1993.

[33] SAWADA H., "Residual electron density study of chromium sesquioxide by crystal structure and scattering factor refinement", *Materials Research Bulletin*, v. 29, n. 3, pp. 239-245, 1994.

[34] MARZOUK, M. A., ELBATAL, F.H., ABDELGHANY, A.M., "Ultraviolet and infrared ab-. sorption spectra of Cr. 2. O. 3. dopedeSodium metaphosphate, lead meta-. phosphate and zinc metaphosphate glasses and effects of gamma irradiation: a comparative study", *Spectrochimica Acta Part A: Molecular and Biomolecular Spectroscopy* v. 114, pp. 658–667, 2013.

[35] MOUSTAFA, F. A., FAYAD, A. M., EZZ-ELDIN, F., *et al*., "Effect of gamma radiation on ultraviolet, visible and infrared studies of NiO, Cr_2O_3 and Fe_2O_3 doped alkali borate glasses", *J. Non-Cryst. Solids*, v. 376, pp. 18-25., 2013.

[36] ANANDAN, N. K., RAJENDRAN, V., "Sheet, spherical and plate-like chromium sesquioxide(Cr_2O_3) nanostructures synthesized via ionic surfactants assisted facile precipitation method", *Materials Letters*, v. 146, pp. 99–102, 2015.

[37] PALERMO, V., SATHICQ, Á.G., VÁZQUEZ, P.G., *et al*., "Doped Keggin heteropolyacids as catalysts in sulfide oxidation", *Reaction Kinetics, Mechanisms and Catalysis*, v. 104, n. 1, pp. 181-195, 2011.

[38] BARTEAU, K., LYONS, J., SONG, I., *et al*., "UV–visible spectroscopy as a probe of heteropolyacid redox properties: application to liquid phase oxidations", *Topics in Catalysis*, v. 41, pp. 55-62, 2006.

ORCID

Valeria Palermo http://orcid.org/0000-0003-2965-5265
María Celeste Gardey Merino http://orcid.org/0000-0002-6616-3545
Patricia Graciela Vazquez https://orcid.org/0000-0002-4196-3976
Jose Antonio Alonso Alonso http://orcid.org/0000-0001-5329-1225
Gustavo Pablo Romanelli http://orcid.org/0000-0002-3529-4753
Mariana Estela Rodriguez Ibarra http://orcid.org/0000-0001-9581-8806
Silvina Lassa https://orcid.org/0000-0001-7194-4664